

## Diameter-Independent Kinetics in the Vapor-Liquid-Solid Growth of Si Nanowires

S. Kodambaka,\* J. Tersoff, M. C. Reuter, and F. M. Ross<sup>†</sup>

IBM Research Division, T. J. Watson Research Center, Yorktown Heights, New York 10598, USA

(Received 7 December 2005; published 9 March 2006)

We examine individual Si nanowires grown by the vapor-liquid-solid mechanism, using real-time *in situ* ultra high vacuum transmission electron microscopy. By directly observing Au-catalyzed growth of Si wires from disilane, we show that the growth rate is *independent of wire diameter*, contrary to the expected behavior. Our measurements show that the unique rate-limiting step here is the irreversible, kinetically limited, dissociative adsorption of disilane directly on the catalyst surface. We also identify a novel dependence of growth rate on wire taper.

DOI: 10.1103/PhysRevLett.96.096105

PACS numbers: 68.65.La, 68.37.Lp, 81.10.-h

Semiconducting nanowires have gained attention recently because of their potential applications in optoelectronics, quantum computing, and sensors [1]. Nanowires are conveniently grown via the vapor-liquid-solid (VLS) process [2], which was first studied four decades ago for Si wires [2–4]. During VLS growth of Si wires, material from the vapor is incorporated via a liquid catalyst, commonly a Si-Au eutectic. This liquid does not wet the Si surface, but instead forms small droplets. Preferential incorporation of Si at these droplets results in cylindrical pillars or “wires” of Si, which can be as narrow as a few nanometers wide and several micrometers long, with wire diameter determined by droplet size.

Although uniform wires with suitable properties have been grown using the VLS process, optimization of nanoscale wires for electronic applications requires a more quantitative understanding of the wire growth mechanism. Particular attention has focused on measurements of the dependence of growth rate on diameter. The classic analysis of Givargizov [4] concluded that narrower wires should grow more slowly due to the Gibbs-Thomson effect, with a critical diameter below which growth cannot occur. However, experimental measurements for Si vary widely. Some work confirms this behavior [4,5]. Other measurements show the opposite [6], with narrower wires growing more rapidly. These differences have been attributed to different growth mechanisms, depending, e.g., on the Si source. While these explanations are quite reasonable, the direct inference of growth mechanism is difficult due to the limitations of postgrowth imaging. Previous *in situ* observations have shown the overall VLS process but have not yielded quantitative kinetics [7].

Here, we present quantitative *in situ* measurement of VLS growth of individual nanowires. We focus on the classic system, Au-mediated growth of Si wires, using disilane ( $\text{Si}_2\text{H}_6$ ) as the Si source. Because wires often taper during growth [8], we are able to follow the growth of individual wires, measuring growth rate as the diameter varies. We can also compare wires of very different diameter growing simultaneously side by side.

Surprisingly, we find *no detectable dependence* of growth rate on wire diameter. We explain the absence of the expected Gibbs-Thomson effect [4] by taking into account the irreversible character of dissociative adsorption. Our measurements and analyses also resolve the question [4] of what is the rate-limiting growth step—under our conditions, the sole rate-limiting step is the dissociative adsorption of disilane on the catalyst surface [3].

As a nanowire tapers, while we see no dependence of growth rate on diameter, we do observe a dependence of growth rate on the *rate of tapering*. This is normally a small correction, but can become dramatic at the termination of wire growth. The dependence arises because the droplet acts as a reservoir of Si, and changes in droplet size correspond to an additional source (or sink) of Si.

Si wire growth experiments are carried out in a multi-chamber ultrahigh vacuum (UHV) system (base pressure  $2 \times 10^{-10}$  Torr) composed of a transmission electron microscope (TEM) with *in situ* physical and chemical vapor deposition facilities [9]. Phosphorous-doped Si(111) wafers with a miscut  $< 0.5^\circ$  and a resistivity  $\leq 0.02 \Omega \text{ cm}$  are used as substrates in our experiments. The samples (1.5 mm wide, 4 mm long, and 0.6 mm thick) are first chemically cleaned, mounted in the microscope with the polished side vertical, and then degassed in UHV at  $600^\circ \text{C}$  for 2 h followed by annealing at  $1250^\circ \text{C}$  for 30 s. Au thin films, 2–3 nm thick, are deposited at room temperature by thermal evaporation from a Knudsen cell at a rate of  $3 \times 10^{-3} \text{ nm/s}$  onto the samples in a preparation chamber at a base pressure of  $2 \times 10^{-8}$  Torr during deposition. The Au-covered Si(111) samples are then transferred under UHV to the microscope, a 300 kV Hitachi H-9000 TEM with base pressure below  $2 \times 10^{-10}$  Torr in the specimen region, and wire growth is initiated by resistively heating the samples in an atmosphere of  $\text{Si}_2\text{H}_6$  (purity 99.999%).

As soon as the samples are heated, the Au film agglomerates into Au-Si eutectic droplets. These act as the catalysts for the formation of individual wires, most of which grow perpendicular to the substrate and hence are imaged with the electron beam perpendicular to the wire axis (Fig. 1). Images are acquired at video rate (30 frames/s).

Growth is observed over a range of  $\text{Si}_2\text{H}_6$  pressures ( $P_{\text{Si}_2\text{H}_6}$ ) from  $1 \times 10^{-8}$ – $1 \times 10^{-5}$  Torr, the maximum pressure being limited to  $10^{-5}$  Torr by the design of the TEM.  $\text{Si}_2\text{H}_6$  was leaked continuously into the microscope column to ensure a constant  $\text{Si}_2\text{H}_6$  pressure during wire growth. A reasonable growth rate can be obtained using temperatures in the range 500–650 °C, with typical growth times between 3 and 6 h. Wires grown under continuous and intermittent electron beam irradiation exhibit similar growth rates, indicating that the electron beam does not affect Si wire growth kinetics. Substrate temperatures are calibrated before and after deposition using an infrared pyrometer. After growth, the surface can be cleaned by heating to 1250 °C, so that a series of growth experiments can be carried out on the same sample at one area. For such a series, the relative temperature can be measured to within 20 °C, while for different samples the measurement uncertainties in absolute temperature are  $\sim 50$  °C.

Figure 1 is a typical bright field TEM image acquired during Si wire growth. Note that all the wires grow in  $\langle 111 \rangle$  directions, with the tips composed of the expected Si-Au eutectic droplets. The  $\langle 111 \rangle$  interface between the Si-Au eutectic and Si stays planar during growth. All the wires are epitaxial and single crystal, with occasional twins on  $\{111\}$  planes. The wire sidewalls are partially faceted into saw-tooth structures [10], which are (barely) visible here. In this particular growth experiment the wire diameters vary between 30 and 135 nm, but this depends on the deposition temperature and on the uncontrolled agglomeration of the Au film that occurs before growth [8].

As seen in Fig. 1, many wires taper visibly. Post-growth observation of tapered wires can reflect direct growth on the sidewall [3,11], with longer exposure giving wider diameter toward the base. However, real-time observations

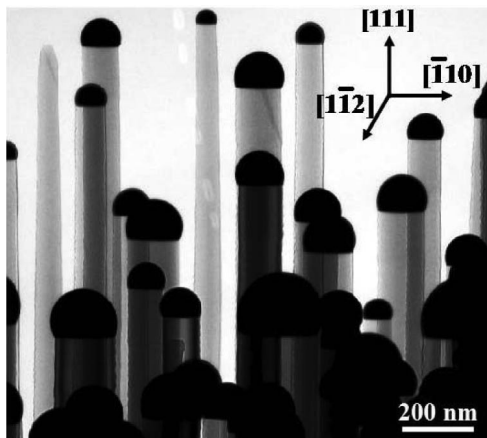


FIG. 1. A typical bright field TEM image obtained from a Si sample during the growth of Si nanowires by the VLS process at a temperature  $T = 575$  °C and disilane pressure  $P_{\text{Si}_2\text{H}_6} = 5 \times 10^{-6}$  Torr. Wires grow in the  $\langle 111 \rangle$  direction and are observed in transmission mode. Because of the limited depth of focus of the image and the large area on which wires grow, many wires seen in the image are out of focus.

confirm that here the catalyst droplet is shrinking over time. This is illustrated in Fig. 2(a), which shows images of a typical Si wire obtained at four successive times during growth at 635 °C and  $1 \times 10^{-6}$  Torr  $\text{Si}_2\text{H}_6$ . In the final image, the droplet disappears and the growth of this wire stops. This shrinking is due to outdiffusion of Au [8], which is itself a very interesting subject; here, it means that we can measure the growth rate of *individual wires as the diameter varies*, with all other factors held constant.

The measured length  $L$  and diameter  $d$  vs time  $t$  are shown for this wire in Fig. 2(b). As the diameter of this wire decreases from 85 to 60 nm over a time of 1200 s, the growth rate  $dL/dt$  of the wire remains constant. It is important to note that the lack of dependence of  $dL/dt$  on  $d$  for an individual wire could only be *directly* determined through real-time monitoring. There is an abrupt change in growth rate between 1200 and 1300 s, when a  $\{111\}$  facet appears on the sidewall. This change is related to the taper angle and not the diameter *per se*, as discussed below.

In addition to examining the dependence of growth rate on diameter for a single wire, we can also compare  $dL/dt$  for an ensemble of neighboring wires imaged simultaneously. Figure 3(a) is a typical plot of  $dL/dt$  vs  $d$ , for wires grown at  $P_{\text{Si}_2\text{H}_6} = 10^{-6}$  Torr and  $T = 655$  °C. Although there is some scatter, there is no systematic dependence on  $d$ . In fact, a least-squares fit to a linear dependence in Fig. 3(a) is virtually horizontal, correspond-

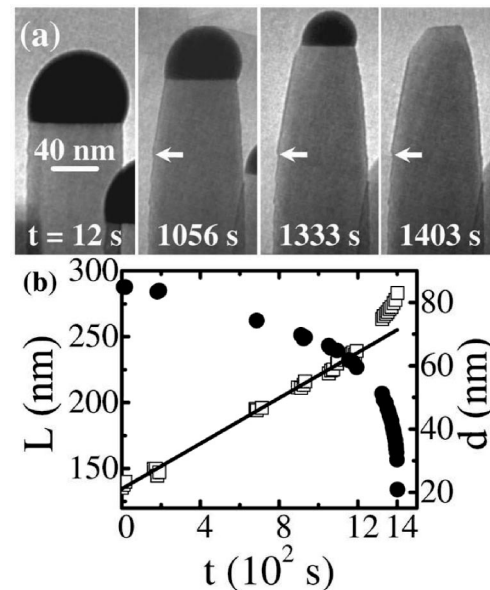


FIG. 2. (a) Representative bright field TEM images of a Si wire acquired at four successive times  $t$  (indicated on the images) during deposition at  $T = 635$  °C and  $P_{\text{Si}_2\text{H}_6} = 1 \times 10^{-6}$  Torr.  $t$  is the time since measurements on this wire began, although growth had been taking place for 4 h 17 min at  $t = 0$ . For clarity, white arrows highlight a reference point on the wire sidewall. (b) Length  $L$  (open squares) and diameter  $d$  (solid circles) of the same wire as a function of  $t$ . The straight line is a least-squares fit to the first 1200 s.

ing to a change of  $<1\%$  in  $dL/dt$  as the wire diameter changes by a factor of 3. Results similar to those shown in Figs. 2 and 3(a) are obtained from measurements of over 50 wires grown under different pressures and temperatures with diameters ranging from 30 to 150 nm. We find that over the lifetime of every wire,  $dL/dt$  does not vary with  $d$ .

The *in situ* observations shown above also allow us to measure the rate of direct growth on the wire sidewall. This is a potentially important source of varying diameter which cannot be distinguished, using postgrowth measurements alone, from a decreasing catalyst droplet size. We find that the noncatalyzed sidewall growth rate for the wire shown in Fig. 2(a) is  $\sim 100$  times slower than  $dL/dt$ .

We now consider the variation in growth rate with pressure and temperature. Figure 3(b) shows  $dL/dt$  plotted as a function of  $P_{\text{Si}_2\text{H}_6}$  at  $T = 575^\circ\text{C}$ . It can be seen that  $dL/dt$  is proportional to  $P_{\text{Si}_2\text{H}_6}$  over 3 orders of magnitude in pressure. Similar results were reported for Si wires grown using  $\text{SiH}_4$  at higher pressures ( $\sim 10^{-1}$  Torr) [12]. The proportionality is related to the reactive sticking probability  $S$  of an incident  $\text{Si}_2\text{H}_6$  molecule. From the data, we can calculate  $S$  using the simple relation  $S = \frac{(dL/dt)A_{\text{wire}}\rho_{\text{Si}}}{2FA_{\text{drop}}}$ , where  $\rho_{\text{Si}}$  is the Si atomic density  $\approx 5 \times 10^{22}$  atoms/cm<sup>3</sup>,  $A_{\text{wire}}$  is the cross-sectional area of the wire,  $A_{\text{drop}}$  ( $\approx 2A_{\text{wire}}$ ) is the surface area of the almost hemispherical droplet, and  $F$  is the  $\text{Si}_2\text{H}_6$  flux (estimated from the measured pressure). For the data in Fig. 3(b), we obtain  $S \approx 0.1$  at  $T = 575^\circ\text{C}$ . The sidewall growth rates are 2 orders of magnitude lower than that of the wires at this  $T$ , giving  $S \sim 10^{-3}$  on the wire sidewalls.

The temperature dependence of  $dL/dt$  is shown in Fig. 3(c). Assuming Arrhenius behavior and using linear least-squares analysis of the data, we obtain an activation energy of  $0.53 \pm 0.02$  eV for the VLS growth of Si wires. Note that the activation energy we obtain is significantly lower than the activation energy of  $\approx 2$  eV associated with the same process on a noncatalyzed Si surface [13].

We can consistently explain all of these observations, including the unexpected diameter-independence of the growth rate, by one simple and natural assumption: that the sole rate-limiting step for wire growth is the thermally

activated Au-catalyzed dissociative adsorption of disilane directly on the catalyst droplet [3]. It has been generally accepted, following the argument of Givargizov [4], that the wire growth rate depends on the supersaturation and, hence, on wire diameter via the Gibbs-Thomson effect. This would be true for growth near equilibrium, or when the growth rate reflects a kinetic competition between Si adsorption and removal, as can occur, e.g., in Si-Cl-H processes [4]. The rate of Si removal does exhibit a Gibbs-Thomson effect, because the Si chemical potential enters in the initial state, so a diameter dependence is expected in this case. However, in our case, as in most systems where VLS growth is studied, adsorption is an irreversible process involving dissociation of the source molecule in a strongly exothermic reaction. Si evaporation is negligible at these temperatures; and there is no reactive ambient to drive desorption. Therefore, the chemical potential of Si in the wire or droplet is irrelevant to the growth rate—for an incident molecule,  $S$  depends only on the probability of being thermally activated over the dissociation barrier. In other words,  $S$  depends on the activation energy to go from the initial state to the transition state; but it does not depend on the final state, which is much lower in free energy. Only the final state is affected by the wire diameter [4,14].

This also answers (for our specific system) another question posed by Givargizov [4]—whether the rate-limiting step is (i) incorporation from the vapor into the liquid, (ii) diffusion through the liquid, or (iii) incorporation from the liquid into the solid. In the absence of Si evaporation, the growth rate is proportional to  $P_{\text{Si}_2\text{H}_6}S$ . Effects (ii) and (iii) both cause the Si chemical potential at the droplet surface to depend on growth rate, and they can affect the growth rate *if and only if* the reactive sticking probability or evaporation rate depend on the Si chemical potential. If, as argued above,  $S$  is independent of the Si chemical potential in the droplet, then neither (ii) nor (iii) can affect the growth rate. We find direct confirmation of this independence from the linear dependence on pressure, Fig. 3(b), which implies constant sticking probability, despite the varying chemical potential. These conclusions do not depend on the low pressure or on the specific

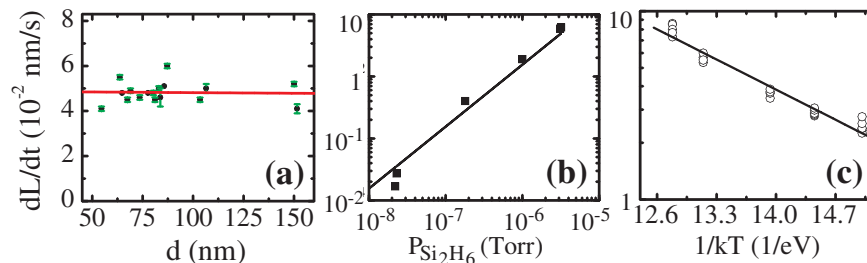


FIG. 3 (color online). (a)  $dL/dt$  vs  $d$  for an ensemble of Si wires grown at  $P_{\text{Si}_2\text{H}_6} = 1 \times 10^{-6}$  Torr and  $T = 655^\circ\text{C}$ . The solid line is a least-squares fit. The error bars represent the measurement uncertainties in growth rates. (b) Log-log plot of  $dL/dt$  of one particular wire grown at varying pressure at a fixed temperature  $T = 575^\circ\text{C}$ . The solid line is the best (least-squares) fit of slope 1. (c) Arrhenius plot of  $dL/dt$  vs  $T$  for 28 wires at  $P_{\text{Si}_2\text{H}_6} = 1 \times 10^{-6}$  Torr. Each data point represents an individual wire. The straight line is the least-squares fit, with an activation energy of  $0.53 \pm 0.02$  eV.

properties of disilane—they should apply in *any* system where growth occurs by irreversible dissociative adsorption on the catalyst [14].

There is another potential source of diameter dependence that is discussed extensively in the literature [15]. If the sticking probability  $S$  is independent of diameter, and sticking occurs only on the catalyst particle (or on any region whose area is proportional to the wire cross-sectional area), the growth rate will be independent of diameter. However, in some systems, material can adsorb onto the wire sidewall or the surface between wires and then diffuse to the catalyst particle, where it is incorporated into the wire. With decreasing wire diameter, the area contributing to growth decreases more slowly than the wire cross-sectional area, giving an *increase* in the linear growth rate. Since our wire growth rate is independent of diameter, we conclude that only molecules *directly incident on the catalyst particle* contribute significantly to wire growth.

Finally, we consider the deviations from uniform growth rate, discussed above in Fig. 2. These variations are an interesting consequence of the wire taper which occurs as a result of Au diffusion from or to the eutectic droplets. For example, in Fig. 2(b) we observe a drastic increase in the growth rate towards the final stage of wire growth, when the droplet is rapidly shrinking. We infer that as the Au diffuses away, the shrinking droplet maintains its composition by depositing excess Si at the liquid-solid interface. This increases the growth rate of the wire. The variation  $\delta$  in linear growth rate due to changes in the droplet volume can be calculated from a simple relationship  $\delta = -f \frac{dV}{dt} / \pi(d/2)^2$ , where  $f$  is the volume fraction of Si in the droplet and  $dV/dt$  is the rate of change of droplet volume. Hence, wires with increasing diameters exhibit a decrease in growth rates while wires with decreasing diameters exhibit accelerated growth rates. The measured variations in growth rate in Fig. 2 and for other strongly tapering wires (not shown) are consistent with the behavior expected for this mechanism.

In conclusion, *in situ* TEM experiments allow us to determine quantitatively the kinetics of Au-catalyzed growth of Si wires under well controlled growth conditions. Our results provide insight into the physical processes controlling the growth of nanowires in the Si/Au system. We find that growth rates are *independent of wire diameter*, and increase linearly with pressure. We show that for wire growth from  $\text{Si}_2\text{H}_6$ , under conditions of low pressure and high temperature, dissociative adsorption of  $\text{Si}_2\text{H}_6$  at the Au-Si droplet surface is the rate-limiting process, with negligible contribution from surface diffusion of Si adsorbed away from the droplet. From the growth rate measurements, we determine the reactive sticking probabilities of  $\text{Si}_2\text{H}_6$  at the droplet surface and at the wire sidewall. We observed a novel dependence of

growth rate on wire taper, which we attribute to the deposition of excess Si from the shrinking droplets.

We acknowledge S. Guha, J. B. Hannon, F. R. McFeely, R. M. Tromp, and P. W. Voorhees for helpful discussions, and A. Ellis for development of the *in situ* microscopy facilities.

---

\*Electronic address: skodamb@us.ibm.com

†Electronic address: fmross@us.ibm.com

- [1] K. Haraguchi *et al.*, Appl. Phys. Lett. **60**, 745 (1992); X. Duan *et al.*, Nature (London) **409**, 66 (2001); M. S. Gudixen *et al.*, Nature (London) **415**, 617 (2002); Y. Cui and C. M. Lieber, Science **291**, 851 (2001); Y. Cui *et al.*, Science **293**, 1289 (2001); J. Wang *et al.*, Science **293**, 1455 (2001); Y. Huang *et al.*, Science **294**, 1313 (2001); M. T. Bjork *et al.*, Appl. Phys. Lett. **81**, 4458 (2002); M. T. Bjork *et al.*, Nano Lett. **4**, 1621 (2004); S. De Franceschi *et al.*, Appl. Phys. Lett. **83**, 344 (2003); S. De Franceschi *et al.*, Appl. Phys. Lett. **83**, 344 (2003); L. Gangloff *et al.*, Nano Lett. **4**, 1575 (2004).
- [2] R. S. Wagner and W. C. Ellis, Appl. Phys. Lett. **4**, 89 (1964); R. S. Wagner *et al.*, J. Appl. Phys. **35**, 2993 (1964); R. S. Wagner, J. Appl. Phys. **38**, 1554 (1967); R. S. Wagner and C. J. Doherty, J. Electrochem. Soc. **113**, 1300 (1966); **115**, 93 (1968); R. S. Wagner in *Crystal Growth* (Pergamon, Oxford and New York, 1967) p. 347.
- [3] G. A. Bootsma and H. J. Gassen, J. Cryst. Growth **10**, 223 (1971).
- [4] E. I. Givargizov and N. N. Sheftal, J. Cryst. Growth **9**, 326 (1971); E. I. Givargizov and A. A. Chernov, Sov. Phys. Crystallogr. **18**, 89 (1973); E. I. Givargizov, J. Cryst. Growth **31**, 20 (1975).
- [5] J. Kikkawa, Y. Ohno, and S. Takeda, Appl. Phys. Lett. **86**, 123109 (2005).
- [6] L. Schubert *et al.*, Appl. Phys. Lett. **84**, 4968 (2004).
- [7] E. A. Stach *et al.*, Nano Lett. **3**, 867 (2003); Y. Wu and P. Yang, J. Am. Chem. Soc. **123**, 3165 (2001); G. Zhou *et al.*, Mater. Res. Soc. Symp. Proc. **737**, F6.3.1 (2003).
- [8] J. B. Hannon, S. Kodambaka, F. M. Ross, and R. M. Tromp, Nature (London) **440**, 69 (2006).
- [9] M. Hammar *et al.*, Surf. Sci. **349**, 129 (1996).
- [10] F. M. Ross, J. Tersoff, and M. C. Reuter, Phys. Rev. Lett. **95**, 146104 (2005).
- [11] J. W. Dailey *et al.*, J. Appl. Phys. **96**, 7556 (2004).
- [12] K.-K. Lew and J. M. Redwing, J. Cryst. Growth **254**, 14 (2003).
- [13] K. Sinniah *et al.*, J. Chem. Phys. **92**, 5700 (1990); T. R. Bramblett *et al.*, J. Appl. Phys. **76**, 1884 (1994).
- [14] In principle, droplet curvature could also affect the transition-state energy; see J. Tersoff, Y. Tu, and G. Grinstein, Appl. Phys. Lett. **73**, 2328 (1998). Similarly, changes in droplet composition could affect the transition state. But these effects can have either sign, and are presumed to be negligible.
- [15] G. W. Sears, Acta Metall. **3**, 361 (1955); J. M. Blakely and K. A. Jackson, J. Chem. Phys. **37**, 428 (1962); V. Ruth and J. P. Hirth, J. Chem. Phys. **41**, 3139 (1964); W. Seifert *et al.*, J. Cryst. Growth **272**, 211 (2004).